CRISPR/Cas9-Based Model of Heterozygous CXCR4$^{WT/R334X}$ Mutation to Study Cellular Phenotypes in WHIM Syndrome

Katarina Zmajkovicova,[1] Sumit Pawar,[2] Sabine Maier-Munsa,[1] Adriana Badarau,[2] Arthur G. Taveras[3]

[1]X4 Pharmaceuticals (Austria) GmbH, Vienna, Austria; [2]Former Employee at X4 Pharmaceuticals (Austria) GmbH, Vienna, Austria; [3]X4 Pharmaceuticals, Inc., Boston, MA, USA

P792

Background

- WHIM (Warts, Hypogammaglobulinemia, Infections, Myelokathexis) syndrome is a rare, autosomal-dominant primary immunodeficiency marked by neutropenia and lymphopenia, and monocytopenia due to impaired leukocyte trafficking.[1-3]
- The pathogenesis of WHIM syndrome is causally linked to heterozygous gain-of-function (GOF) mutations predominantly in the C-terminus of the chemokine receptor CXCR4, a master regulator of immune cell trafficking and homeostasis, causing receptor desensitization defects and hyperactivation of downstream signaling.[3,4]
- c.1000C>T is the most frequently reported mutation in patients with WHIM syndrome, which results in a premature C-terminal truncation of the receptor at position R334 (R334X).[3]
- Primary cells isolated from patients with the R334X variant display CXCR4 receptor internalization defects and GOF phenotypes in signaling assays.[5]
- The GOF cellular phenotypes of WHIM syndrome can be modeled in *in vitro* assays using cell lines with exogeneous overexpression of *CXCR4*^{WHIM} variants but may not entirely mimic the condition in patients, who typically are heterozygous and have 1 wild-type (WT) *CXCR4* allele.[5]
- Mavorixafor, a CXCR4 antagonist, is currently being evaluated in a global phase 3 clinical trial for the treatment of patients with WHIM syndrome (NCT04274738).[6,7]

Objectives

- This study aimed to characterize a cellular model of homozygous and heterozygous CXCR4^{R334X} in the endogenous locus, to better understand the pathogenic impact of harboring mutations in 1 or both alleles.

Methods

- CRISPR/Cas9 platform was used to establish a model of heterozygous mutations found in patients with WHIM syndrome.
- Jurkat cell line (with endogenous expression of *CXCR4*^{WT}) was edited to harbor the c.1000C>T/R334X mutation in a single allele (RX/WT; clone B2) or in both alleles (RX/RX; clones A3 and B5).
- Unedited parental Jurkat cell line and Jurkat cells with edited silent mutations (WT/WT; clone C3) were used as controls.

Results

Heterozygous (RX/WT) and homozygous (RX/RX) mutants display CXCR4 receptor trafficking defect

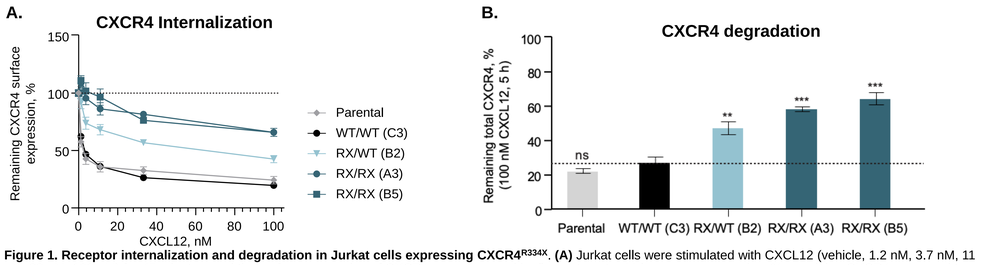

Figure 1. Receptor internalization and degradation in Jurkat cells expressing CXCR4^{R334X}. (A) Jurkat cells were stimulated with CXCL12 (vehicle, 1.2 nM, 3.7 nM, 11 nM, 33 nM, 100 nM) for 45 minutes, and the surface expression of CXCR4 was measured by flow cytometry. Values are expressed as % remaining CXCR4 compared to vehicle-treated cells. Values represent mean +/- SEM, n=6. **(B)** Jurkat cells were stimulated with vehicle or 100 nM CXCL12 for 5 hours, and the whole-cell lysates were analyzed by western blot to determine total CXCR4 levels. Values represent % of treated sample compared to vehicle control. Mean +/- SEM, n=4. CXCL12, C-X-C chemokine ligand 12; ns, not significant; WT, wild-type. *P* values <.05 were considered statistically significant and set as follows: **—*P*<.01; ***—*P*<.001.

- Upon stimulation with C-X-C chemokine ligand 12 (CXCL12), RX/WT-expressing cells had an intermediate internalization defect (43% of CXCR4 receptors remaining on the cell surface at 100 nM CXCL12) compared to RX/RX cell lines (65%), parental (24%), and WT lines (20%).
- Once internalized, the CXCR4 receptor is predominantly sorted to lysosomes and degraded. This was the case in cells having CXCR4^{WT}, in which the total levels of the receptor decreased by 73%–78% after 5 hours' incubation with 100 nM CXCL12. RX/RX variants showed impaired CXCR4 degradation (36%–42% decrease), and the RX/WT cells again displayed intermediate effects (53% decrease) in the degradation assay.

Heterozygous (RX/WT) and homozygous (RX/RX) mutants exhibit enhanced CXCL12-induced calcium mobilization and increased extracellular signal-regulated kinase (ERK) activation

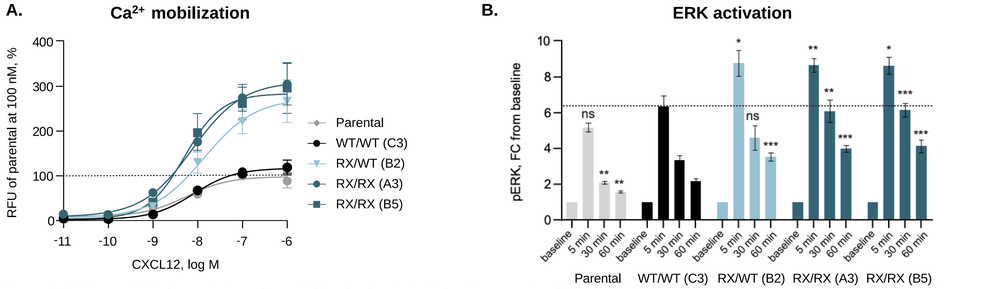

Figure 2. Calcium mobilization and downstream ERK activation in Jurkat cells expressing CXCR4^{R334X}. (A) Jurkat cells were stimulated with serial dilutions of CXCL12 to measure Ca^{2+} mobilization. RFU measured in parental line at 100 nM CXCL12 represented 100%. Mean +/- SEM, n=4. **(B)** Jurkat cells were stimulated with 10 nM CXCL12 for 5, 30, or 60 minutes; fixed and the median fluorescence intensity of p-T202/Y204 ERK staining was measured by flow cytometry. Values are expressed as FC compared to unstimulated sample. Mean +/- SEM, n=6–7. ERK, extracellular signal-regulated kinase; FC, fold change; ns, not significant; pERK, phosphorylated extracellular signal-regulated kinase; RFU, relative fluorescent unit; WT, wild-type. *P* values <.05 were considered statistically significant and set as follows: *—*P*<.05; **—*P*<.01; ***—*P*<.001.

Table 1. An Overview of CXCL12-Induced Ca^{2+} Mobilization in Parental, WT, and R334X-Expressing Cells

Cell line	Ca^{2+} mobilization	
	EC_{50} (nM ± SE)	E_{max} (% ± SE)
Parental	5.6 ± 2.7	98 ± 7.5
WT/WT (C3)	8.1 ± 3.2	117 ± 9.2
RX/WT (B2)	13.8 ± 9.5	273 ± 40
RX/RX (A3)	7.6 ± 4.5	310 ± 34
RX/RX (B5)	5.1 ± 3.1	283 ± 28

CXCL12, C-X-C chemokine ligand 12; EC_{50}, half maximal effective concentration; E_{max}, maximum effect; WT, wild-type.

- Calcium mobilization in response to CXCL12 was enhanced in cells harboring the R334X mutation, reaching a 2.5- to 3-fold higher maximum effect compared to cells with *CXCR4*^{WT}.
- ERK activation downstream of CXCR4 reached a higher amplitude (8-fold increase over baseline) and duration after stimulation with CXCL12 in all lines expressing R334X compared to the parental and WT/WT cell lines (6-fold increase).
- Presence of a single mutant allele seemed to confer the full GOF phenotype in both signaling readouts in this cell line.

R334X-expressing cells exhibit enhanced chemotaxis

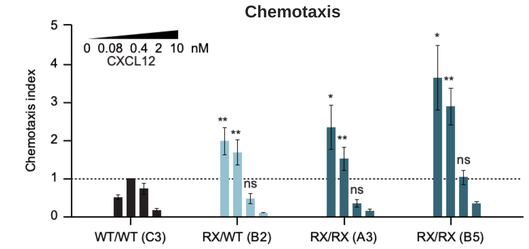

Figure 3. Chemotaxis of Jurkat cells upon stimulation with CXCL12.
Jurkat cells were subjected to trans-well chemotaxis assay. Cells migrated toward 0.08, 0.4, 2, and 10 nM CXCL12 or medium only for 2 hours. The total number of migrated cells was normalized to WT with 0.4 nM CXCL12 in each assay. Mean +/- SEM, n=4. CXCL12, C-X-C chemokine ligand 12; ns, not significant; WT, wild-type. *P* values <.05 were considered statistically significant and set as follows: *—*P*<.05; **—*P*<.01.

- The 2 homozygous clones showed different chemotactic responses (A3 was comparable to RX/WT and B5 migrated more than RX/WT); therefore, we were not able to conclude on the differences between heterozygous and homozygous mutations.

Mavorixafor was active in an unbiased manner on a spectrum of CXCR4-related functions

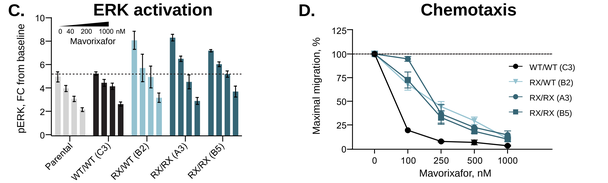

Table 2. An Overview of Response to Mavorixafor in Parental, WT, and R334X-Expressing Cells

Cell line	CXCL12 binding inhibition	Ca^{2+} mobilization	Chemotaxis
	IC_{50} (nM ± SE)	IC_{50} (nM ± SE)	IC_{50} (nM ± SE)
Parental	1.9 ± 0.09	1.5 ± 0.9	-
WT/WT (C3)	1.6 ± 0.12	0.7 ± 0.3	30 ± 10
RX/WT (B2)	2.4 ± 0.07	3.4 ± 3.6	366 ± 334
RX/RX (A3)	2.1 ± 0.1	5 ± 2.8	188 ± 20
RX/RX (B5)	1.9 ± 0.15	2 ± 1.2	153 ± 23

CXCL12, C-X-C chemokine ligand 12; ns, not significant; IC_{50}, half maximal inhibitory concentration; WT, wild-type.

Figure 4. Functional analysis and sensitivity to mavorixafor in Jurkat cells expressing CXCR4^{R334X}. (A) Jurkat cells were pretreated with serial dilutions of mavorixafor, incubated with AF647-CXCL12, and subjected to flow cytometry to determine the ligand binding inhibition potency of mavorixafor. Mean +/- SEM, n=4. **(B)** Jurkat cells were preincubated with serial dilutions of mavorixafor and then stimulated with 100 nM CXCL12. Mean +/- SEM, n=4–10, **(C)** Profiling of mavorixafor in ERK activation assays. K562 cells with stable *CXCR4* expression were preincubated with vehicle, 40 nM, 200 nM, or 1 µM mavorixafor and then stimulated with 10 nM CXCL12 for 5 min. Median fluorescence intensity of p-T202/Y204 ERK staining was measured by flow cytometry. Values are expressed as FC compared to unstimulated cells. SEM, n=6–8. **(D)** Profiling of mavorixafor in chemotaxis assays. Jurkat cells were preincubated with vehicle, 100 nM, 250 nM, 500 nM, or 1 µM mavorixafor and subjected to migration toward 0.4 nM CXCL12. % maximal migration was determined with respect to the vehicle-pretreated sample. Mean +/- SEM, n=3. When statistics are indicated, samples were compared to WT/WT (C3) clone for the respective conditions. CXCL12, C-X-C chemokine ligand 12; ERK, extracellular signal-regulated kinase; FC, fold change; ns, not significant; pERK, phosphorylated extracellular signal-regulated kinase; RFU, relative fluorescent unit; WT, wild-type.

Conclusions

- This is the first study to establish a cellular model recapitulating the heterozygous CXCR4$^{WT/R334X}$ mutations found in patients with WHIM syndrome using the CRISPR/Cas9 platform.
- The established cellular model recapitulates the functional defects found in immune cells from patients with WHIM syndrome.
- When stimulated with CXCL12, WT/RX-expressing cells appeared to display full GOF phenotype in downstream signaling assays, including enhanced calcium mobilization and increased ERK activation, compared to RX/RX-expressing cells, which is consistent with the dominant inheritance pattern of WHIM syndrome.
- These results bring several novel insights in *CXCR4*^{WHIM} biology and enriches the toolbox of models available for studying WHIM syndrome.

References

1. Wetzler M, et al. *Am J Med*. 1990;89:663-672. **2.** McDermott DH, et al. *N Engl J Med*. 2019;380:163-170. **3.** Heuskinveld LE, et al. *J Clin Immunol*. 2019;39(6):532-556. **4.** Balabanian K, et al. *Blood*. 2005;105(6):2449-2457. **5.** McDermott DH, et al. *J Cell Mol Med*. 2011;15(10):2071-2081. **6.** NIH. Clinicaltrials.gov NCT04274738. February 18, 2020. Updated August 17, 2021. Accessed April 27, 2022. https://clinicaltrials.gov/ct2/show/record/NCT04274738?term=04274738&draw=2&rank=1&view=record. **7.** Dale DC, et al. *Blood*. 2020;136(26):2994-3003.

Acknowledgements

The authors would like to thank Harald Rouha for initiating the generation of R334X-edited cell lines, and PRECISIONscientia in Yardley, PA, USA, for medical writing assistance, which was supported financially by X4 Pharmaceuticals in compliance with international Good Publication Practice guidelines.

Disclosures

SP and **AB** are former employees of X4 Pharmaceuticals and/or have equity ownership of X4 Pharmaceuticals. **KZ, SMM,** and **AGT** are current employees and/or have equity ownership of X4 Pharmaceuticals.